Choi *et al. Journal of Biological Engineering* (2025) 19:103
https://doi.org/10.1186/s13036-025-00573-1

Journal of Biological Engineering

RESEARCH Open Access

# Integration of TLR7/8 agonists into lipid nanoparticles enhances antigen-specific immune responses to N1-methyl-Ψ-modified mRNA-LNP vaccines

Huijeong Choi[1,2†], Seonghyun Lee[1,2†], Hyejin Kim[3,4,5], Seo-Hyeon Bae[1,2], Sohee Jo[1,2], Jungmin Kim[1,2], Yeeun Lee[1,2], Dahyeon Ha[1,2], Ayoung Oh[1,2], Subin Yoon[1,2], Sanghyuk Jeon[1,2], Yu-Sun Lee[1,2], Youngran Cho[1,2], Seongje Cho[1], Gahyun Roh[1], Sowon Lee[1,2], Jayaraj Gowda[3,4], Hyo-Jung Park[1,2], Jisun Lee[1], Daesub Song[6], So-Hee Hong[7], Soo Bong Han[3,4*] and Jae-Hwan Nam[1,2,8*]

## Abstract

N1-methylpseudouridine (N1-methyl-Ψ)-modified mRNA offers a safer alternative to unmodified mRNA-based cancer immunotherapies but induces weaker innate immune responses. This study aimed to enhance the expression of N1-methyl-Ψ-modified mRNA and improve innate and adaptive immune responses by incorporating a toll-like receptor (TLR) 7/8 agonist (AD7/8) into a lipid nanoparticle (LNP). AD7/8 was incorporated into LNPs by partially replacing cholesterol, and the mRNA expression efficiency of various formulations was evaluated, leading to the selection of the LNP formulation containing 0.5% AD7/8 (AD03-LNP). AD03-LNP was evaluated using mRNAs encoding human papillomavirus (HPV)16 E7 and HPV18 E6 antigens, the SARS-CoV-2 Omicron spike protein (S-Omicron), and influenza hemagglutinin (HA), and it consistently enhanced antigen-specific immune responses compared with conventional LNP. In the HPV mRNA model, antigen-specific $CD8^+$ T cell and cytokine responses were significantly increased by 1.5-2.1-fold. In the S-Omicron mRNA model, IgG2a levels, indicative of a Th1-skewed response, were markedly elevated by 8-fold as measured by endpoint titers. Importantly, in the HA mRNA model, which evaluated both cellular and humoral immunity, AD03-LNP induced significantly higher $CD8^+$ T cell responses by 2.3-2.6-fold, together with increased antibody production, with total IgG elevated by 3.6-fold as measured by endpoint titers. These findings demonstrate that AD03-LNP enhances both cellular and humoral immune responses across diverse antigens. These results provide insights into how TLR7/8 agonist-loaded LNPs influence mRNA expression and immune responses, supporting an effective formulation approach to boost the immunogenicity of

[†]Huijeong Choi and Seonghyun Lee contributed equally to this work.

*Correspondence:
Soo Bong Han
sbhan@krict.re.kr
Jae-Hwan Nam
jhnam@catholic.ac.kr

Full list of author information is available at the end of the article

© The Author(s) 2025. **Open Access** This article is licensed under a Creative Commons Attribution-NonCommercial-NoDerivatives 4.0 International License, which permits any non-commercial use, sharing, distribution and reproduction in any medium or format, as long as you give appropriate credit to the original author(s) and the source, provide a link to the Creative Commons licence, and indicate if you modified the licensed material. You do not have permission under this licence to share adapted material derived from this article or parts of it. The images or other third party material in this article are included in the article's Creative Commons licence, unless indicated otherwise in a credit line to the material. If material is not included in the article's Creative Commons licence and your intended use is not permitted by statutory regulation or exceeds the permitted use, you will need to obtain permission directly from the copyright holder. To view a copy of this licence, visit http://creativecommons.org/licenses/by-nc-nd/4.0/.

mRNA-LNP vaccines. This approach may help advance the design of mRNA-based cancer immunotherapies and prophylactic vaccines that depend on strong T cell responses.

**Keywords** Toll-like receptor 7/8 agonist, Lipid nanoparticles, mRNA vaccine

## Background

mRNA vaccines represent a promising immunotherapeutic strategy, as they enable the induction of antigen-specific immune responses through the delivery of mRNA encoding a target antigen, typically formulated with a delivery system [1]. However, when non-self mRNA is introduced into the body exogenously, the innate immune system often recognizes it as a pathogen-associated molecular pattern. This recognition can reduce mRNA stability and translational efficiency, which could limit the effectiveness of mRNA-based vaccines [2]. To address the limitations of mRNA instability and innate immunogenicity, nucleobase modifications such as the incorporation of N1-methylpseudouridine (N1-methyl-Ψ) have been introduced that enhance RNA stability, reduce immune activation, and improve protein expression [3–5]. These modifications enable mRNA to evade immune detection, thereby reducing the activation of RNA-dependent protein kinase (PKR) and preventing the induction of type I interferons (IFNs) [5, 6], ultimately enhancing their stability and translational efficiency [7]. Notably, N1-methyl-Ψ has been pivotal in overcoming the limitations of mRNA vaccines, especially in the context of coronavirus disease 2019 (COVID-19) vaccines [8]. It enhances translation and suppresses innate immunity, ultimately contributing to high vaccine efficacy [2, 7, 8].

Despite these N1-methyl-Ψ usage-associated benefits, type I IFNs remain key molecules that activate antigen-presenting cells (APCs) and promote T cell immunity [9]. A deficiency in type I IFN signaling has been associated with severe disease progression in COVID-19, highlighting its crucial role in improving T cell responses for effective treatment [10]. In cancer vaccine immunotherapy, unmodified mRNA vaccines have effectively inhibited tumor growth and metastasis by promoting IFN-I production and signaling, thereby eliciting a robust antitumor T cell response [11]. Wild-type uridine-5′-triphosphate (UTP) mRNA is susceptible to translational inhibition through the PKR/eukaryotic translation initiation factor 2 alpha signaling pathway; however, N1-methyl-Ψ-modified mRNA circumvents this immune response and promotes ribosome recruitment, leading to enhanced protein expression [3]. Therefore, while N1-methyl-Ψ-modified mRNA is preferred over wild-type UTP mRNA for its enhanced translation and stability, additional strategies are needed to augment innate and T cell responses.

Recent studies have reported that lipid-modified toll-like receptor (TLR) 7/8 agonist incorporated into mRNA-LNPs enhances innate immunity while preserving protein expression, thereby promoting robust antigen-specific responses [12, 13]. TLRs are pattern recognition receptors critical for activating cell-mediated immune responses in the innate immune system [14]. Specifically, TLR7/8 activation enhances T helper type 1 (Th1) immune responses through nuclear factor kappa B (NF-κB) signaling, which promotes pro-inflammatory cytokine [tumor necrosis factor-alpha (TNF-α), interleukin (IL)-12, IFN-gamma (γ)] secretion, and type I IFN signaling, which induces $CD8^+$ T cell proliferation and cytokine production [15]. In addition, TLR7/8 agonists bind to TLR7/8 and induce high levels of cytokines critical for promoting Th1 immune responses, while simultaneously activating conventional and plasmacytoid dendritic cells [16, 17]. This process strengthens $CD8^+$ T and natural killer cell functionality, driving specific adaptive immune responses and increasing cytotoxicity against cancer cells [18]. The addition of TLR7/8 agonists to LNPs requires adjustments in nanoparticle composition to preserve efficient mRNA delivery. In this context, reducing the cholesterol content has been shown to facilitate intracellular delivery and improve extrahepatic targeting, thereby enhancing mRNA delivery to the spleen or other tissues [19, 20].

This study aimed to develop a clinically relevant mRNA–LNP vaccine by incorporating a TLR7/8 agonist into an SM-102–based formulation. To achieve this, a portion of the cholesterol was replaced with the TLR7/8 agonist, enabling enhanced intracellular delivery and spleen delivery while sustaining mRNA expression and eliciting both innate and adaptive immune responses.

## Methods

### Materials

SM-102 was purchased from Hanmi Fine Chemical Co., Ltd. (Siheung, Republic of Korea). Cholesterol, 1,2-distearoyl-sn-glycero-3-phosphocholine (DSPC), and 1,2-dimyristoyl-rac-glycero-3-methoxypolyethylene glycol-2000 (DMG-PEG) were purchased from Avanti Polar Lipids (Alabaster, AL, USA). Hybrid-2 [21], a conventional TLR7/8 agonist and imidazoquinoline analogue derived from R848 (Resiquimod), and a novel TLR7/8 agonist (AD7/8) were synthesized by the Korea Research Institute of Chemical Technology (KRICT; Daejeon, Republic of Korea). The full structural details and synthetic route of AD7/8, a TLR7/8 agonist with a bicyclic

core containing an R-substituted position, are not disclosed due to ongoing patent considerations. The AD7/8 has the chemical formula $C_{21}H_{33}N_7O$ and a molecular weight of 399.54 (Fig. S1A). The AD7/8 showed an $EC_{50}$ of 1.63 μM (Emax 1.65, $CC_{50}$ >100 μM) for TLR7 and an $EC_{50}$ of 0.011 μM (Emax 1.71, $CC_{50}$ >100 μM) for TLR8 (Fig. S1B). The identity and purity of AD7/8 were verified by LC–MS and HPLC. LC/MS (ESI) m/z calculated for $C_{21}H_{33}N_7O$: 399.54, found: 400.52, calculated for [M + H]+: 400.54 (Fig. S1C). The purity of compound AD7/8 was confirmed to be greater than 99% by reverse-phase UPLC analysis performed on a Waters Acquity H-Class system equipped with a photodiode array (PDA) detector (Fig. S1D). The separation was achieved using a linear gradient of 10% to 90% acetonitrile in water.

#### Mice and ethics statement

The Institutional Animal Care and Use Committee (IACUC) of the Catholic University of Korea (Approval No. CUK-IACUC-2023-048-02) approved all animal experiments. Six-week-old female C57BL/6, Institute for Cancer Research (ICR), and BALB/c mice were obtained from Dae-Han Bio-Link (Chungbuk, Republic of Korea) and Koatech (Pyeongtaek, Republic of Korea). The experimental animals were housed under specific pathogen-free conditions in a controlled environment at 22 °C with a 12/12-hour light/dark cycle. All data in this study were obtained and analyzed in accordance with the ethical guidelines of the Institutional Animal Care and Use Committee (IACUC), and all procedures complied with the NIH (National Research Council) Guide for the Care and Use of Laboratory Animals as well as relevant national regulations to minimize animal suffering. A total of 173 mice were used in this study. Sample sizes were determined a priori using a non-parametric Wilcoxon–Mann–Whitney analysis [22] (two-sided $\alpha = 0.05$; power = 0.80). Based on pilot variability (SD ≈ 5) and an expected difference of 20 (d = 4), $n = 5$ per group was chosen as a conservative size. For the luciferase activity assay, group size was determined by the number of available ears ($n = 3–4$). Mice were randomly assigned to experimental groups, and data analysis was performed in a blinded manner to reduce bias.

#### QUANTI-blue secreted embryonic alkaline phosphatase (SEAP) assay

HEK-Blue human TLRs (hTLR7 and hTLR8) cells were seeded in 96-well plates. The cells were incubated in a 37 °C incubator with 5% CO2. The cells were treated with increasing concentrations of AD7/8 and commercial TLR agonists, including Vesatolimod (GS-9620), Selgantolimod (GS-9688), and Resiquimod (R848), which served as positive controls. Then, the culture medium was collected and transferred to a 96-well plate, and QUANTI-Blue™ (InvivoGen) was added to each well. SEAP activity was quantified at OD 620 nm.

#### NF-κB activity luciferase assay using pNF-κB-luciferase reporter

RAW264.7 cells were seeded at $5 \times 10^5$ cells per well and transfected with 0.3 μg of phosphorylated NF-κB-luciferase reporter plasmid (631904, Clontech, Mountain View, CA) using Lipofectamine 2000 (Thermo Fisher Scientific, Waltham, MA, USA), per manufacturer's instructions. AD7/8 was added at 5 μg/well after 3 h. As positive controls, cells were treated with 5 μg/well of Hybrid-2 and 2 μg/well of lipopolysaccharide. After 24 h of treatment, cells were lysed using Cell Culture Lysis 5X Reagent (Promega, Madison, WI, USA), and luciferase activity was measured using the Luciferase 1000 Assay System (Promega) per the manufacturer's protocol. Luminescence was measured using a GloMax® Explorer (Promega).

#### Preparation of mRNA

mRNAs encoding Renilla luciferase (Rluc), human erythropoietin (hEPO), and Firefly luciferase (Fluc) were used in evaluating in vivo protein expression. mRNA sequences encoding human papillomavirus (HPV) 16 E7 and HPV18 E6 antigens, the hemagglutinin (HA) of influenza A virus (A/Puerto Rico/8/1934), and the spike protein of the severe acute respiratory syndrome coronavirus 2 (SARS-CoV-2) Omicron variant were used to assess immune responses. All protein-coding sequences were cloned into plasmid vectors designed as an mRNA vaccine platform, which included a T7 promoter, muscle-specific 5′ and 3′ untranslated regions, and a 100-nucleotide poly(A) tail flanked by a 20-nucleotide A50LA50 linker [23]. The plasmid vectors were then linearized with *NotI* restriction enzyme (Enzynomics, Daejeon, Republic of Korea) and transcribed in vitro using the EZ™ T7 High-Yield In Vitro Transcription Kit (Enzynomics) following the manufacturer's protocol. Capping of the CUK3–1 mRNA platform was conducted using SC101 (STPharm, Republic of Korea), with UTP replaced by N1-methyl-Ψ (TriLink BioTechnologies, San Diego, CA, USA). Residual DNA was digested using RNase-free DNase I (Enzynomics). The transcribed mRNAs were then precipitated with lithium chloride at – 20 °C, washed with 70% ethanol, and resuspended in sterile distilled water. To reduce double-stranded RNA (dsRNA) contamination, cellulose-based purification was applied as a secondary step. The efficiency of dsRNA removal was assessed using dot blot analysis with poly I: C (Sigma-Aldrich, USA) as a dsRNA-positive control and a J2 dsRNA-specific mouse monoclonal antibody (Jena Bioscience, Thuringia, Germany) for detection. RNA quality and size were evaluated

through agarose gel electrophoresis using a RiboRuler High-Range RNA Ladder (Thermo Fisher Scientific).

#### Formulation of mRNA-loaded lipid nanoparticles

Control lipid nanoparticles were formulated with the Moderna lipid formulation [ionizable lipids (SM-102), phospholipids (DSPC), cholesterol, and PEGylated lipids (DMG-PEG2000); 50:10:38.5:1.5 mol%]. Experimental LNPs that incorporated AD7/8 were designed using the same lipid components as the Con-LNPs but with modified cholesterol ratios to allow AD7/8 inclusion. Before the mRNA-LNPs formulation, a lipid mixture was prepared by dissolving ionizable lipids (SM-102), cholesterol, phospholipids (DSPC), and PEGylated lipids (DMG-PEG2000) in a chloroform/methanol mixture (1:1, v/v). AD7/8 was separately dissolved in dimethyl sulfoxide and added to the film preparation. All the components were combined at the molar ratios indicated in Supplementary Tables 1 and subsequently concentrated under reduced pressure. mRNA-loaded LNPs were formulated using the enCELL-Master V2 system (ENPARTICLE, Busan, Korea) by mixing the ethanol-dissolved lipid mixture with mRNA dissolved in citrate buffer (pH 4.0, 50 mM) at a 1:3 volume ratio. The neutron-to-proton ratio (proportional to the mol% of ionizable lipids) was fixed at 6 for all LNP formulations. The resulting LNPs were concentrated by ultrafiltration using an Amicon Ultra centrifugal filter (UFC9030; Merck Millipore, Billerica, MA, USA) and subjected to buffer exchange with Dulbecco's phosphate-buffered saline (DPBS).

#### Characterization of mRNA-loaded lipid nanoparticles

For particle size and polydispersity index (PDI) measurements, mRNA-loaded LNP solutions were diluted 200-fold in DPBS. For zeta potential analysis, samples were diluted in ultrapure water. Particle size, PDI, and zeta potential measurements were conducted using a PANalytical Zetasizer Ultra (Malvern Panalytical, Malvern, UK), utilizing Ratiolab HRA-2,722,120 cuvettes for size and PDI, and folded capillary zeta cells (DTS1070) for zeta potential.

The Quant-iT™ RiboGreen RNA Assay Kit (Invitrogen, Thermo Fisher Scientific, Carlsbad, CA, USA) was used to assess the mRNA encapsulation efficiency (EE%) of the LNPs. Standard mRNA solutions were prepared by serial dilution of the mRNA stock solution in 1× tris(hydroxymethyl)aminomethane-ethylenediaminetetraacetic acid (TE) buffer. mRNA-loaded LNP solutions were diluted 300-fold in 1× TE buffer to quantify unencapsulated mRNA. Conversely, the total mRNA content (encapsulated and free) was determined by lysing the LNPs in 1× TE buffer containing 0.5% Triton X following a 300-fold dilution. RiboGreen dye was added to all samples in a 96-well black plate, and fluorescence intensities were measured between 500 and 550 nm using a GloMax® Explorer (Promega, WI, USA), with an excitation wavelength of 475 nm. mRNA concentrations were calculated using a standard curve, and the EE% was determined accordingly.

#### Luciferase activity assay for in vivo expression analysis

The in vivo Rluc expression was assessed following intradermal (ID) administration into the ears of the six-week-old ICR mice. The mice were anesthetized with 5% isoflurane, and 20 μL of LNPs encapsulating 5 μg of Rluc mRNA was injected into the ear skin using a 30G insulin syringe (BD, NJ, USA). At 6 h post-injection, mice were euthanized, and both ear tissues and whole blood were collected. The tissues were minced and homogenized in Renilla lysis buffer. Luciferase activity was quantified using the Rluc Assay System after brief centrifugation (Promega, WI, USA) following the manufacturer's instructions. Luminescence was measured using the GloMax® Explorer.

#### Human erythropoietin expression analysis

LNPs (40 and 100 μL), each encapsulating 5 μg of hEPO mRNA intramuscularly (IM) and intravenously (IV), respectively, were injected into the C57BL mice. After 3 h, the mice were euthanized, and serum was collected for analysis. The hEPO levels were measured using a hEPO DuoSet enzyme-linked immunosorbent assay (ELISA) kit (DY286, R&D Systems, USA) following the manufacturer's specifications.

#### Bioluminescence imaging of mRNA expression for biodistribution analysis

Bioluminescence imaging (BLI) was conducted using LUCI (Neoscience, Chungbuk, Republic of Korea) to examine the distribution of Fluc mRNA expression across the tissues. For IM and IV administration, 40 and 100 μL of LNPs, each encapsulating 10 μg of Fluc mRNA, were injected into six-week-old C57BL mice. D-luciferin (Promega, Madison, WI, USA) was administered intraperitoneally at a dose of 3 mg per mouse as the luciferase substrate. The mice were euthanized 5 min post-injection, and major organs, including the liver, spleen, lungs, heart, and lymph nodes, were harvested for ex vivo imaging. Bioluminescence images reflecting Fluc mRNA expression were obtained at the same time points under identical imaging conditions across all groups. BLI signals were recorded using LUCI (Neoscience) and analyzed using NEOimage software (Neoscience, v5.2.6).

#### Immunization with human papillomavirus mRNA-lipid nanoparticles

Female C57BL mice were initially divided into four groups ($n = 5$) to compare the immune responses elicited

by different LNP-formulated mRNA vaccines. Following these results, the most immunogenic formulation was selected for further analysis. The mice were then divided into three groups ($n = 5$) following the same immunization protocol and were immunized with mRNA encoding the HPV16 E7 and HPV18 E6 antigens (10 μg, IM). The immunization schedule included a prime dose followed by a booster dose administered 1 week later. Mice were sacrificed 1 week post-booster immunization to collect whole blood and spleens. The serum was isolated by allowing the blood to clot at room temperature for 2 h, followed by centrifugation.

#### Immunization with spike protein of severe acute respiratory syndrome coronavirus 2 Omicron mRNA-lipid nanoparticles

Female BALB/c mice were randomly divided into three groups ($n = 5$) to receive the LNP-formulated mRNA vaccine. The mice were immunized with mRNA encoding the spike protein of the SARS-CoV-2 Omicron (S-omicron) variant (10 μg, IM). The immunization schedule included a prime dose followed by a booster 2 weeks later. The mice were sacrificed 2 weeks post-booster immunization to collect whole blood. The serum was isolated by allowing the blood to clot at room temperature for 2 h, followed by centrifugation.

#### Immunization with hemagglutinin mRNA-LNPs

Female BALB/c mice were randomly divided into three groups ($n = 5$) for LNP-formulated mRNA vaccine administration. The mice were immunized with mRNA encoding the HA sequence of influenza A/Puerto Rico/8/1934 (H1N1; 10 μg, IM). The immunization schedule included a prime dose followed by a booster 2 weeks later. The mice were sacrificed 1 week post-booster immunization to collect whole blood and spleens. The serum was isolated by allowing the blood to clot at room temperature for 2 h, followed by centrifugation.

#### Antigen-specific immunoglobulin G Enzyme-linked immunosorbent assay

ELISA was conducted to assess the levels of antigen-specific IgG1 and IgG2a in mouse serum. A 96-well plate was coated overnight at 4 °C with either HA or S-omicron spike protein (both from Sinobiological, Beijing, China) [100 ng/100 μL per well]. Subsequently, the wells were blocked with 1% bovine serum albumin in phosphate-buffered saline (PBS, 100 μL/well) for 1 h at room temperature. Serum samples, diluted in blocking buffer, were added to the wells and incubated for 2 h at room temperature. For HA-specific ELISA, serum dilutions ranged from 1/50–1/100,000,000, while for S-omicron spike protein-specific ELISA, the dilution range was 1/400–1/1,638,400. The plates were washed three times with PBS containing Tween 20 (PBS-T), after which horseradish peroxidase-conjugated anti-mouse total IgG (Bethyl Laboratories, Montgomery, TX, USA), IgG1 (Bethyl Laboratories), or IgG2a (Bio-Rad, Hercules, CA, USA) antibodies were added. Following a 1-hour incubation at room temperature, the wells were washed again and developed with 3,3′,5,5′-tetramethylbenzidine substrate for 15 min. The reaction was stopped with 2 N sulfuric acid, and the absorbance was measured at 450 nm using the GloMax® Explorer.

#### Cytokine enzyme-linked immunosorbent assay

Monocyte chemoattractant protein-1 (MCP-1), IFN-γ, and IL-6 levels in serum samples collected from mice after intradermal (ID) injection of Rluc mRNA-LNPs, respectively, were measured to evaluate the innate immune activation and immunostimulatory potential of LNPs. The samples were diluted 1:5 and 1:3 in ELISA/enzyme-linked immunospot (ELISPOT) diluent (1X). MCP-1, IFN-γ, and IL-6 concentrations were determined using an ELISA kit (Invitrogen, Thermo Fisher Scientific Inc.) following the manufacturer's instructions.

To quantify cytokine secretion by antigen-stimulated splenocytes, harvested splenocytes from immunized mice were plated at $5 \times 10^5$ cells / well in 96-well plates. The cells were stimulated for 24 h at 37 °C with a peptide mixture consisting of HPV16 E7 (RAHYNIVTF, 2 μg/mL) and HPV18 E6 (KCIDFYSRI, 2 μg/mL). Peptides were synthesized by Peptron (Daejeon, Korea) with ≥ 95% purity. IFN-γ, TNF-α, IL-6, and IL-2 levels were quantified in the culture supernatants using ELISA kits (Invitrogen) following the manufacturer's protocols. Cytokine levels were calculated based on standard curves and expressed as picograms per milliliter (pg/mL).

#### Enzyme-linked immunospot assay

Splenocytes from immunized mice were cultured at $5 \times 10^5$ cells / well in 96-well MultiScreen-IP filter plates (Millipore). The cells were stimulated with the same HPV16 E7 and HPV18 E6 peptide mixture (2 μg/mL each) for 36 h at 37 °C. IFN-γ ELISPOT assays were conducted using a mouse IFN-γ detection kit (Cat. 3321–2 A, Mabtech, Stockholm, Sweden) following the manufacturer's instructions. The peptides were also synthesized by Peptron (Daejeon, Korea) with ≥ 95% purity.

#### Flow cytometry

Splenocytes were initially blocked with anti-mouse CD16/32 antibody (Biolegend) for 20 min at 4 °C and then stained with flow cytometry antibodies and LIVE/DEAD™ Fixable Aqua Dead Cell Stain (405 nm excitation) for 30 min at 4 °C in the dark. The stained cells were fixed with 4% paraformaldehyde. For intracellular cytokine staining, splenocytes were stimulated with either the

HPV16 E7/HPV18 E6 peptide mixture or a HA-specific T cell epitope peptide pool (IYSTVASSL, LYEKVKSQL, DYEELREQL, SFERFEIFPKE, HNTNGVTAACSH, KLKNSYVNKKGK, NAYVSVVTSNYNRRF, and CPKYVRSAKLRM; 2.5 μg/well), followed by treatment with Brefeldin A (GolgiPlug, BD Biosciences) and Monensin (GolgiStop, BD Biosciences) for 12 h at 37 °C. After blocking, cells were surface-stained as previously described, permeabilized using a Fixation/Permeabilization Solution Kit (BD Biosciences) for 50 min at 4 °C, and subsequently stained with intracellular antibodies for 30 min at 4 °C (both in the dark). Cells were analyzed using a CytoFLEX flow cytometer (Beckman Coulter), and CytExpert software (Beckman Coulter) was used to process data. The details of all flow cytometry antibodies are listed in Supplementary Tables 2–3. All peptides were synthesized by Peptron (Daejeon, Korea) with ≥ 95% purity.

#### Hemagglutination inhibition assay

The hemagglutination inhibition (HI) assay was conducted per World Health Organization guidelines described in the *'Manual for the Laboratory Diagnosis and Virological Surveillance of Influenza'.* Mouse sera were treated with receptor-destroying enzyme (Denka Seiken, Tokyo, Japan) at 37 °C overnight and subsequently heat-inactivated at 56 °C for 30 min. Serial two-fold serum dilutions were prepared in PBS in V-bottom 96-well plates and incubated with standardized influenza virus (4 HA units/25 μL) for 1 h at room temperature (18–25 °C). Subsequently, 1% chicken red blood cells were added, and the plates were incubated at room temperature (18–25 °C) for 1 h. HI titers were defined as the reciprocal of the highest serum dilution that completely inhibited hemagglutination in duplicate wells and expressed as geometric mean titers. For titers below the detection threshold (1:10), a value of 1:5 was assigned for data analysis.

#### Toxicological analysis

Serum samples were collected 7 days following the second IM injection of HPV mRNA-LNPs. The samples were analyzed by the ©KPNT (Chungbuk, Republic of Korea) using a Biochemistry panel. Alanine aminotransferase (ALT), aspartate aminotransferase (AST), total bilirubin (T-Bil), and creatinine (Crea) serum levels were measured to monitor liver and kidney function. Complete blood counts [Red Blood Cell (RBC), Hemoglobin (HGB), Hematocrit (HCT), Reticulocyte (Retic), Platelet (PLT), and White Blood Cell (WBC)] were analyzed using an automated hematology analyzer by ©KPNT (Chungbuk, Republic of Korea). Whole blood samples were collected 7 days after the second IM injection of HA mRNA-LNPs under isoflurane anesthesia into EDTA-coated tubes (e.g., Microtainer®, BD Biosciences). Whole blood samples were collected from five mice per group. Samples showing substantial clotting were excluded from all hematological assessments.

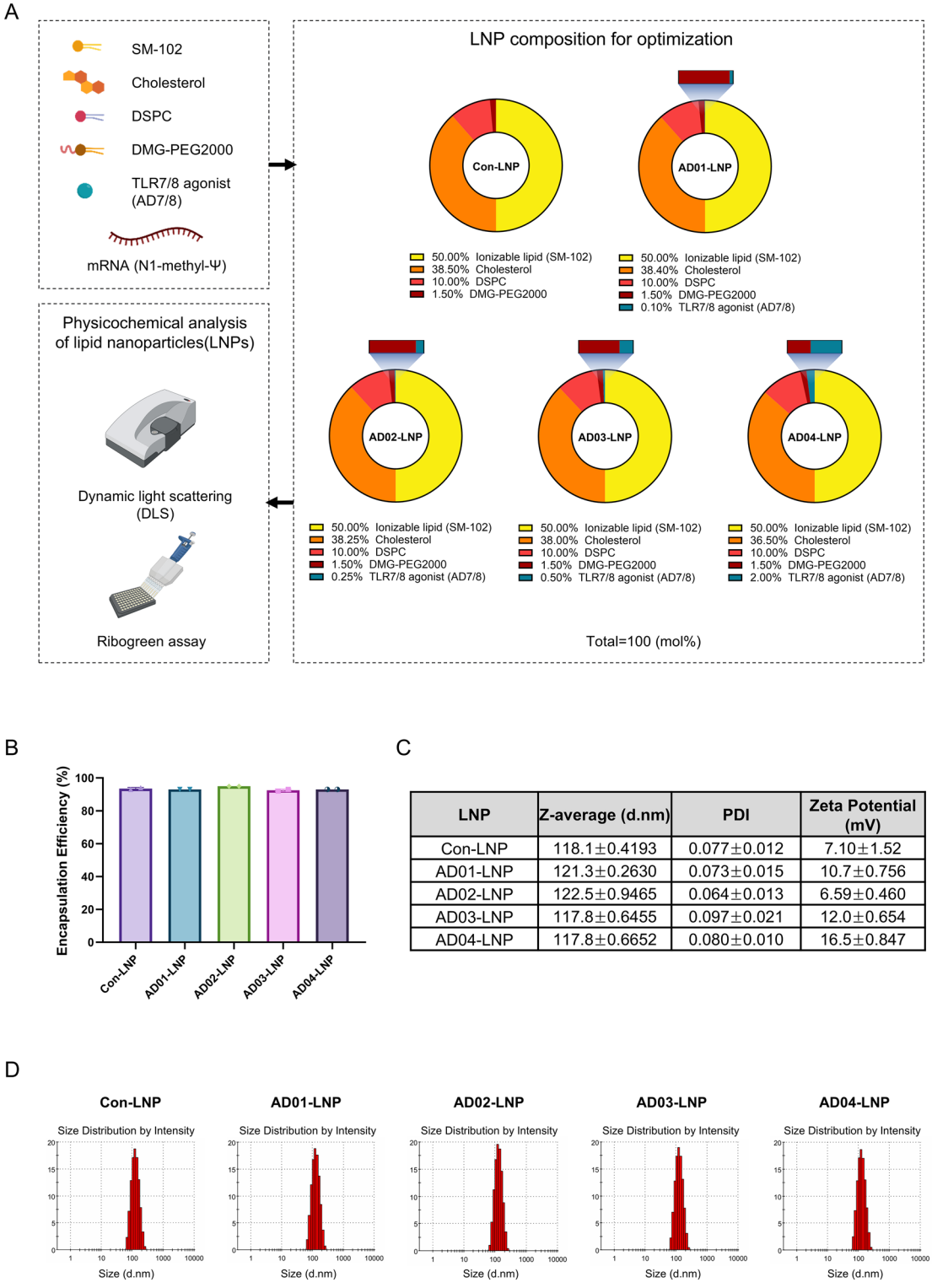
#### Statistical analysis

Prism 10.0.3 software (GraphPad Software, San Diego, CA, USA) was used to conduct all statistical analyses. The data are presented as mean ± standard deviation (SD). Multiple comparisons between experimental groups were conducted using one-way or two-way analysis of variance (ANOVA). For some data, statistical comparisons between two groups were conducted using an unpaired two-tailed Student's t-test. Statistically significant differences were defined as $^{*}P < 0.05$, $^{**}P < 0.01$, $^{***}P < 0.001$, and $^{****}P < 0.0001$.

## Results

#### Composition and physicochemistry of formulated lipid nanoparticle with mRNA and toll-like receptor 7/8 agonists

The novel TLR7/8 agonist AD7/8 is a small molecule with the chemical formula $C_{21}H_{33}N_7O$ and a molecular weight of 399.54, containing a bicyclic core structure with an R-substituted position (Fig. S1A). Functional evaluation using HEK-Blue™ reporter assays revealed that AD7/8 exhibited a markedly TLR8-biased profile ($EC_{50}$ = 0.011 μM for hTLR8, 1.63 μM for hTLR7), in contrast to R848, which showed only modest TLR8 selectivity ($EC_{50}$ = 5.71 μM for hTLR8, 0.127 μM for hTLR7) (Fig. S1B). This pharmacological selectivity suggests that AD7/8 has the potential to drive stronger TLR8-dependent Th1-type immune responses compared to conventional TLR7/8 agonists [24]. The in vitro activation of the NF-κB signaling pathway by TLR7/8 agonists was confirmed using the pNF-κB-luciferase reporter system. In this system, endogenous NF-κB binds to NFκB enhancer elements to induce Fluc gene transcription (Fig. S2). The positive control lipopolysaccharide (LPS) activated NF-κB signaling via TLR4, while both Hybrid-2 [21], a conventional TLR7/8 agonist and an imidazoquinoline analogue derived from R848 (Resiquimod), and the novel TLR7/8 agonist AD7/8 effectively triggered NF-κB activation as part of their TLR7/8 agonistic activity (Fig. S2). Unlike LPS and Hybrid-2, the AD7/8 showed a marked reduction in NF-κB-luciferase activity at 48 h compared to 24 h, indicating a transient activation of NF-κB signaling. This temporal pattern shows a lower potential for prolonged inflammation and systemic toxicity (Fig. S2). Following these results, the TLR7/8 agonist, AD7/8, was mixed with lipid components and mRNA, then formulated using microfluidics, similar to standard mRNA-LNPs, with several compositions [**Control LNP (Con-LNP)**, **AD01-LNP**, **AD02-LNP**, **AD03-LNP**, **AD04-LNP;** Fig. 1A]. As the proportion of the TLR7/8 agonist increased, the




| LNP | Z-average (d.nm) | PDI | Zeta Potential (mV) |
|---|---|---|---|
| Con-LNP | 118.1±0.4193 | 0.077±0.012 | 7.10±1.52 |
| AD01-LNP | 121.3±0.2630 | 0.073±0.015 | 10.7±0.756 |
| AD02-LNP | 122.5±0.9465 | 0.064±0.013 | 6.59±0.460 |
| AD03-LNP | 117.8±0.6455 | 0.097±0.021 | 12.0±0.654 |
| AD04-LNP | 117.8±0.6652 | 0.080±0.010 | 16.5±0.847 |

**Fig. 1** Physicochemical characterization of mRNA-lipid nanoparticles with variable toll-like receptor 7/8 agonist incorporation. (**A**) Scheme summarizes the composition of various lipid nanoparticles (LNPs) and the physicochemical characterization of mRNA-LNPs using dynamic light scattering (DLS) and RiboGreen assays. (**B**) Encapsulation efficiency (EE%) was determined using the RiboGreen assay by comparing the fluorescence of free mRNA and total mRNA. (**C**) Size, polydispersity index (PDI), and zeta potential of mRNA-LNPs were measured using DLS. Each formulation was analyzed in triplicate. (**D**) Size distributions with peak diameters centered around 100–110 nm. (**B**, **C**) Data are shown as mean ± standard deviation

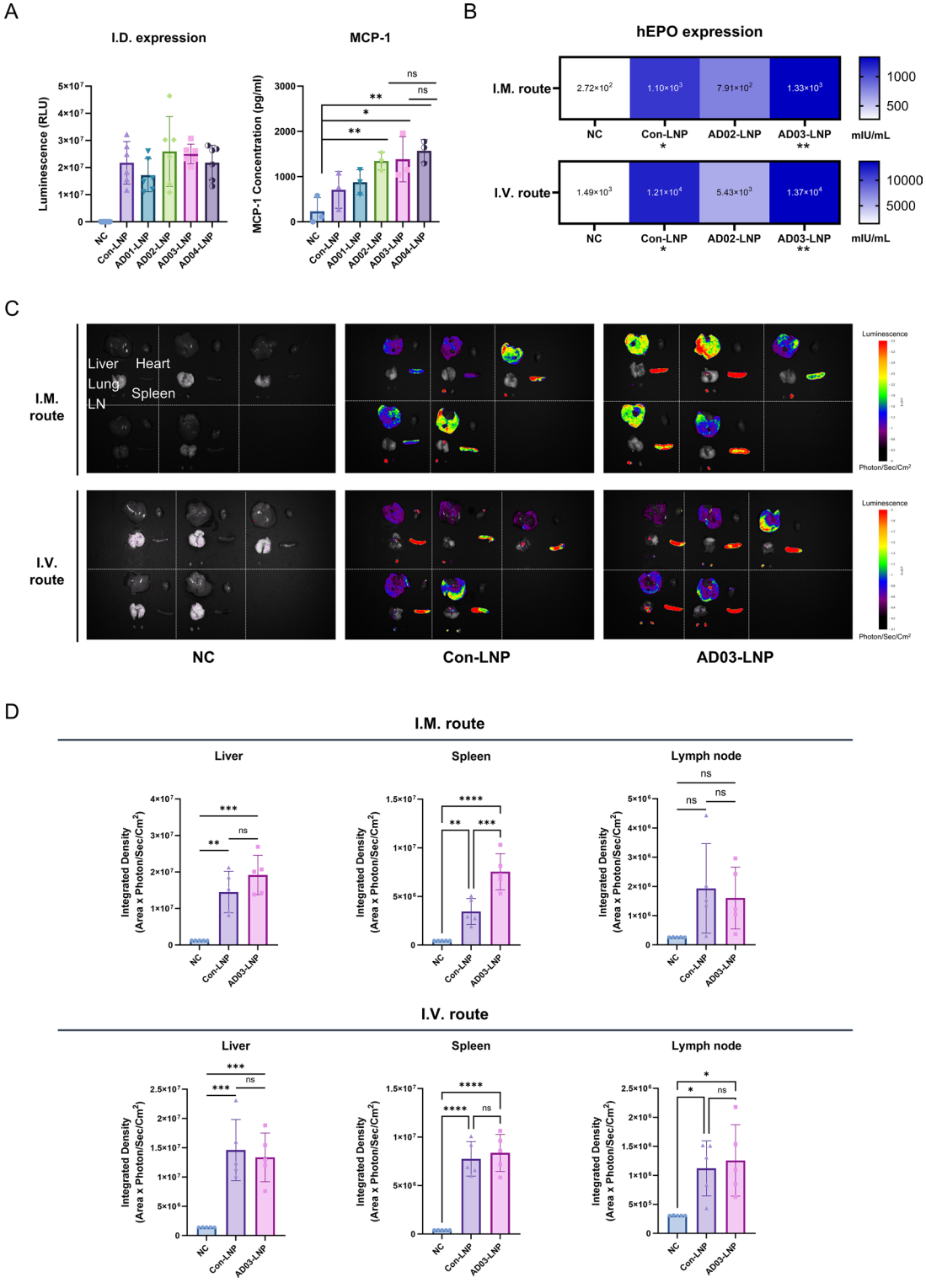



**Fig. 2** (See legend on next page.)

cholesterol content was proportionally reduced at a 1:1 ratio. To confirm how TLR7/8 agonists inclusion altered physiochemistry, each formulation was evaluated for size, polydispersity index (PDI), and zeta potential using dynamic light scattering (DLS) and for encapsulation efficiency (EE%) using the Ribogreen assay (Fig. 1A). All formulations showed similar EE%, indicating that adding TLR7/8 agonists did not significantly influence mRNA

(See figure on previous page.)

**Fig. 2** Expression efficiency of mRNA-lipid nanoparticles via intradermal, intramuscular, and intravenous routes. **(A)** Quantification of luciferase activity 6 h after intradermal (ID) administration of 5 μg Renilla luciferase (Rluc) mRNA-lipid nanoparticles (LNPs) in ICR/6 female mice ($n = 3$ per group). Serum monocyte chemoattractant protein-1(MCP-1) levels were measured using enzyme-linked immunosorbent assay at 6 h post-injection. **(B)** Human erythropoietin (hEPO) levels were measured 6 h after 5 μg hEPO mRNA-LNPs injection via intramuscular (IM) and intravenous (IV) routes in C57BL/6 mice ($n = 5$ per group). **(C-D)** Ex vivo bio-distribution of AD03-LNP. C57BL/6 mice ($n = 5$ per group) were injected with 10 μg Firefly luciferase (Fluc) mRNA-LNPs via IM and IV routes. Luciferase signals were assessed in the liver, spleen, lymph nodes, lungs, and heart. **(D)** Bio-distribution analysis of the IM and IV injection showed a Fluc bioluminescence signal in the liver and spleen lymph node (LN). **(A**, **B**, **D)** All data are shown as the mean ± standard deviation. All *P*-values are determined using an unpaired t-test **(A)** or one-way analysis of variance **(B, D)**. *P*-values are relative to the NC group **(B)** or to all groups **(D)**. $^{*}P < 0.05$, $^{**}P < 0.01$, $^{***}P < 0.001$

encapsulation (Fig. 1B). Furthermore, the LNP size and PDI also showed no difference among the formulations (Fig. 1C, D). Zeta potential values for all formulations remained within an acceptable range (Fig. 1C). All formulations exhibited no significant alterations in size, PDI, and EE% after 14 days of storage at 4 °C (Fig. S3A-B), and remained stable for 7 days when stored at − 80 °C–25 °C (Fig. S3C-F). Additionally, long-term physicochemical stability was evaluated using the mRNA-LNPs employed in subsequent experiments (Fig. 5) and showed no significant changes in size, PDI, and EE% during storage at 4 °C (Fig. S2). Overall, incorporating TLR7/8 agonists into the mRNA-LNPs formulation did not affect its physicochemical properties but preserved its stability.

#### Expression efficiency of each formulation with/without toll-like receptor 7/8 agonist in vivo

Renilla luciferase (Rluc) activity and human erythropoietin (hEPO) expression were evaluated in mice following intradermal (ID), intravenous (IV), and intramuscular (IM) administration. This study aimed to assess the impact of different LNP formulations on expression efficiency. All LNP formulations showed efficient expression following ID administration (Fig. 2A). To evaluate the immunostimulatory effects of each LNP formulation, serum Monocyte chemoattractant protein-1 (MCP-1) levels in samples collected from the same mice subjected to Rluc analysis were measured. A modest increase in circulating MCP-1 levels in AD02-LNP, AD03-LNP, and AD04-LNP groups was observed (Fig. 2A). Given the comparable MCP-1 levels and expression profiles across these three formulations, it was concluded that the amount of TLR7/8 agonist used in AD03-LNP was sufficient, as further increases did not provide additional benefit.

Consequently, AD02-LNP and AD03-LNP were selected for further evaluation in the hEPO expression assay. The mice received Con-LNP, AD02-LNP, or AD03-LNP via IM or IV injection. The group injected with DPBS was used as the negative control (NC) group. Among the LNP-treated groups, Con-LNP and AD03-LNP induced significantly higher hEPO expression (1100 mIU/ml and 1330 mIU/ml for the IM route, 12100 mIU/ml and 13700 mIU/ml for the IV route) than the NC group (272 IU/ml and 1490 IU/ml for the IM and IV routes, respectively), while AD02-LNP showed a modest, non-statistically significant increase in hEPO levels (Fig. 2B). Additionally, a slight expression increase was observed in Con-LNP and AD03-LNP relative to AD02-LNP, with no significant difference between Con-LNP and AD03-LNP. This suggests that incorporating a defined amount of the TLR7/8 agonist in the LNP formulation did not negatively affect either the physicochemical properties or the actual expression efficiency (Fig. 2B). This finding is significant, as TLR7/8 agonists have been associated with concerns about possibly reducing the expression efficiency due to the induction of type I IFN responses. Notably, AD03-LNP elicited higher antigen-specific immune responses than both Con-LNP and AD02-LNP, leading to its selection as the final TLR7/8 agonist-containing LNP formulation (Fig. S5).

While hEPO expression levels were comparable between the Con-LNP group and the AD03-LNP group following IV injection, a modest increase was observed in the AD03-LNP group after IM injection. Whether this discrepancy resulted from differences in systemic biodistribution or tissue-specific expression was then investigated. To address this, an ex vivo biodistribution study was conducted using Fluc mRNA delivered via both routes. AD03-LNP also showed a slight increase in the luminescence signal in major organs compared with Con-LNP following IM administration; however, no such difference was observed with IV administration (Fig. 2C). Overall, adding a TLR7/8 agonist to the mRNA-LNPs formulation resulted in promising in vivo expression levels across all injection routes without any reduction. Importantly, IM administration of AD03-LNP led to significantly higher luminescence signals in the spleen than Con-LNP (Fig. 2D). The spleen, being rich in immune cells, including T cells, B cells, and dendritic cells, represents a key site for immune activation; thus, the elevated expression of AD03-LNP in this organ shows a strong potential to enhance immune responses.

After confirming that incorporating the TLR7/8 agonist did not affect mRNA expression efficiency, the innate immune response and protein expression were evaluated by administering Con-LNP or AD03-LNP formulated with either wild-type UTP mRNA or N1-methyl-Ψ-modified mRNA through ID injection. Rluc activity was measured to assess expression, and serum cytokine levels

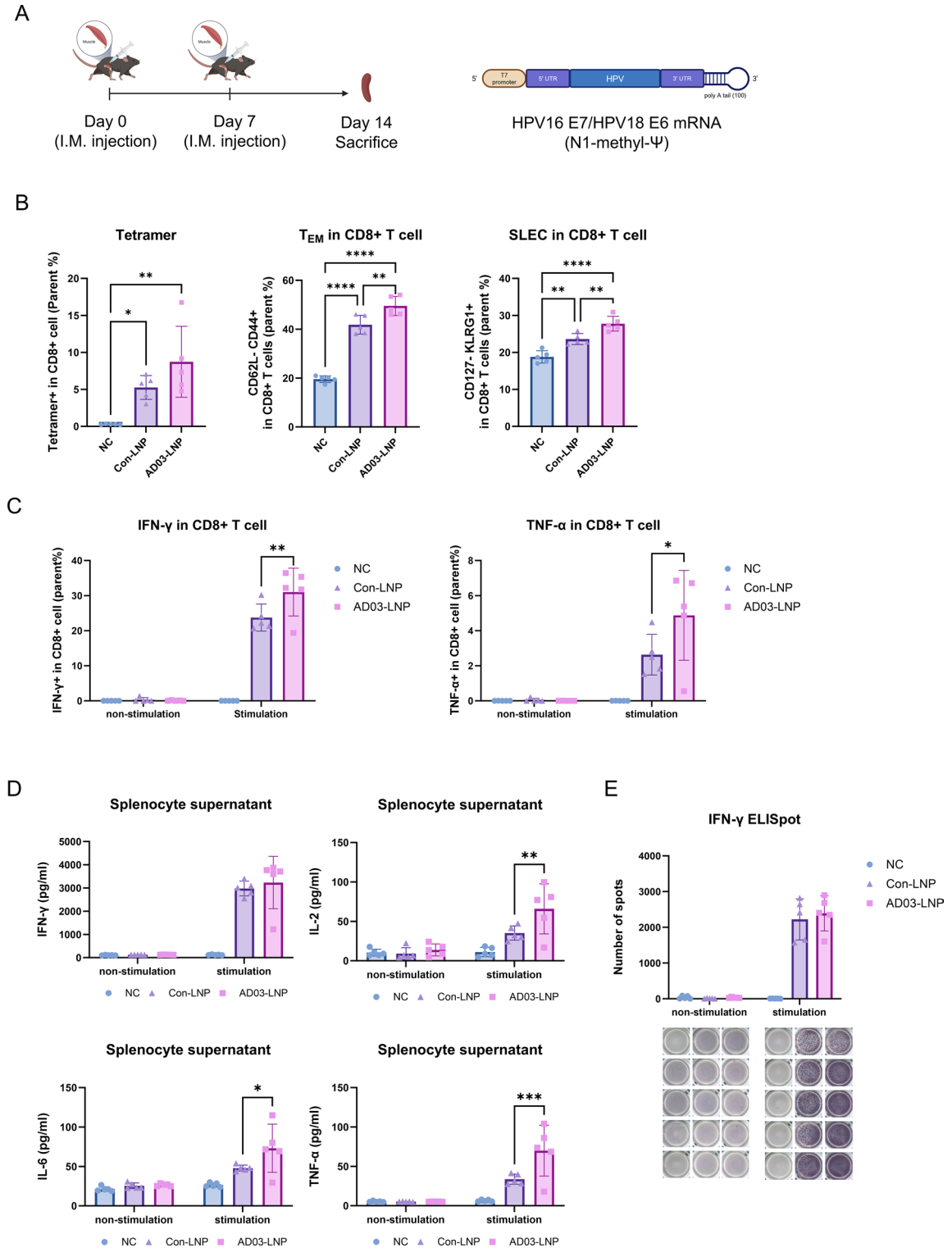



**Fig. 3** (See legend on next page.)

from the same animals were quantified. Compared to the N1-methyl-Ψ-modified mRNA group, the wild-type UTP mRNA showed a significant reduction in Rluc expression (Fig. S6A). Furthermore, the serum levels of MCP-1, IFN-γ, and IL-6 were significantly elevated in the wild-type UTP group, showing an increased risk of systemic inflammatory toxicity (Fig. S6B). Conversely, within the N1-methyl-Ψ-modified mRNA group, treatment with

(See figure on previous page.)

**Fig. 3** Immune responses and T cell activation marker analysis via flow cytometry and enzyme-linked immunospot. **(A)** Schematic of the immunization schedule. C57BL/6 female mice ($n = 5$ per group) were injected intramuscularly with 10 μg of HPV mRNA-LNPs on day 0 (prime) and boosted on day 7. Spleens were collected on day 14 for analysis. **(B)** The parent percentage of E749-57 tetramer + $CD8^+$ T -cells, effector memory T cell ($T_{EM}$; $CD62L^-$, $CD44^+$) in $CD8^+$ T cells, and short-lived effector cells (SLEC; $CD127^-$, $KLRG1^+$) in $CD8^+$ T cells. **(C)** The parent percentage of interferon (IFN)-$\gamma^+$ cells and tumor necrosis factor (TNF)-$\alpha^+$ cells in $CD8^+$ T cells. **(B–C)** Data were obtained via flow cytometry analysis of the spleen. **(D)** Cytokine (IFN-γ, TNF-α, interleukin (IL)-2, IL-6) levels in splenocyte supernatants were measured using cytokine enzyme-linked immunosorbent assay. **(E)** Quantitative plot and images of IFN-γ levels measured using an enzyme-linked immunospot (ELISPOT) assay. Splenocytes ($5 \times 10^5$ cells) were cultured in 96-well plates. **(C–E)** All stimulation groups were stimulated with a peptide mixture consisting of human papillomavirus (HPV) 16 E7 (RAHYNIVTF, 2 μg/mL) and HPV18 E6 (KCIDFYSRI, 2 μg/mL). **(B–E)** All data are shown as the mean ± standard deviation. All *P*-values were determined using a one-way analysis of variance (ANOVA) **(B)** or two-way ANOVA **(C–E)**. *$P < 0.05$, **$P < 0.01$, ***$P < 0.001$, and ****$P < 0.0001$

AD03-LNP resulted in a significant ~ 4.9-fold increase in IFN-γ ($p < 0.05$) and a trend toward elevated MCP-1 levels (~ 1.6-fold, $p = 0.0539$) compared to Con-LNP, while IL-6 showed no significant increase ($p = 0.0954$) (Fig. S6B). These results show that AD03-LNP enhances immunogenicity without triggering excessive inflammatory cytokine responses while preserving the high expression efficiency conferred by N1-methyl-Ψ-modified mRNA.

### Toll-like receptor 7/8 agonist-integrated LNP mRNA vaccine enhances T cell responses

The results from MCP-1 and IFN-γ ELISA (Fig. S6B) showed enhanced innate immune activation by TLR7/8 agonist-containing LNPs; however, whether this translated into improved antigen-specific T cell responses remains unclear. To address this, the mice were immunized twice with each LNP formulation via IM injection at one-week intervals. One week after the final immunization, splenocytes were analyzed using flow cytometry, an enzyme-linked immunospot (ELISPOT) assay, and a cytokine sandwich ELISA. The human papillomavirus (HPV)16 E7 and HPV18 E6 antigens sequence was inserted between the 5′ and 3′ UTRs in the mRNA and transcribed using N1-methyl-Ψ (Fig. 3A). Mice immunized with AD03-LNP showed a statistically significant increase in effector memory T cells ($T_{EM}$) and short-lived effector cells (SLEC) within the $CD8^+$ T cell population compared with the Con-LNP or NC groups. This indicates that AD03-LNP effectively enhances cellular immune responses (Fig. 3B). Furthermore, AD03-LNP immunization resulted in a slight increase in HPV-specific $CD8^+$ T cells as measured by tetramer staining; however, the difference was not statistically significant. Upon stimulation with an HPV antigen-specific peptide, $CD8^+$ T cells from the AD03-LNP group secreted significantly higher IFN-γ and TNF-α levels than those from other groups, suggesting that the AD03-LNP enhances antigen-specific immune reactivity (Fig. 3C). Additionally, the cytokine ELISA showed that splenocytes from the AD03-LNP group produced higher IL-2, IL-6, and TNF-α levels upon stimulation with an HPV peptide than those from the other groups, consistent with the flow cytometry findings (Fig. 3D). However, IFN-γ levels showed no significant difference between the Con-LNP and AD03-LNP groups in either the cytokine ELISA or ELISPOT assay (Fig. 3D, E). These findings show that AD03-LNP enhances cellular immune responses and improves antigen-specific reactivity.

### Toll-like receptor 7/8 agonist-integrated LNP mRNA vaccine did not compromise humoral responses

Given that strong antigen-specific T cell responses may dampen humoral immunity, humoral immune responses were next assessed. This evaluation was conducted by inserting the spike protein of the SARS-CoV-2 Omicron variant (S-Omicron) into the mRNA platform and administering IM, with or without a TLR agonist, to mice at two-week intervals for two doses. Two weeks after the final injection, the serum samples were collected and analyzed for various immunoglobulin G (IgG) levels and neutralizing antibody responses (Fig. 4A). No significant differences were observed in total IgG, IgG1, or neutralizing antibody titers between the Con-LNP and AD03-LNP groups (Fig. 4B, C). However, AD03-LNP showed statistically higher IgG2a levels, which commonly represent Th1 responses, than Con-LNP, suggesting that AD03-LNP mainly stimulates T cell responses (Fig. 4C).

### Concurrent evaluation of cellular and humoral immunity induced by toll-like receptor 7/8 agonist-integrated LNP mRNA vaccination

In previous experiments (Fig. 4), only humoral immune responses were assessed without parallel evaluation of $CD8^+$ and $CD4^+$ T cell responses. To determine whether the TLR7/8 agonist-integrated LNP mRNA vaccine could concurrently induce a robust $CD8^+$ T cell response without compromising the induction of antigen-specific antibodies, a comprehensive analysis of cellular and humoral immunity within a single experimental setting was conducted. This approach allowed us to directly assess whether enhanced CD8 T cell activation is accompanied by preserved levels of IgG, IgG subclass, and neutralizing antibody responses following immunization. Female BALB/c mice aged 6 weeks were immunized twice with mRNA encoding the HA sequence of influenza A/Puerto Rico/8/1934 (HA mRNA) at two-week intervals and were sacrificed one week after the final immunization (Fig. 5A). Compared to the Con-LNP group, the AD03-LNP group

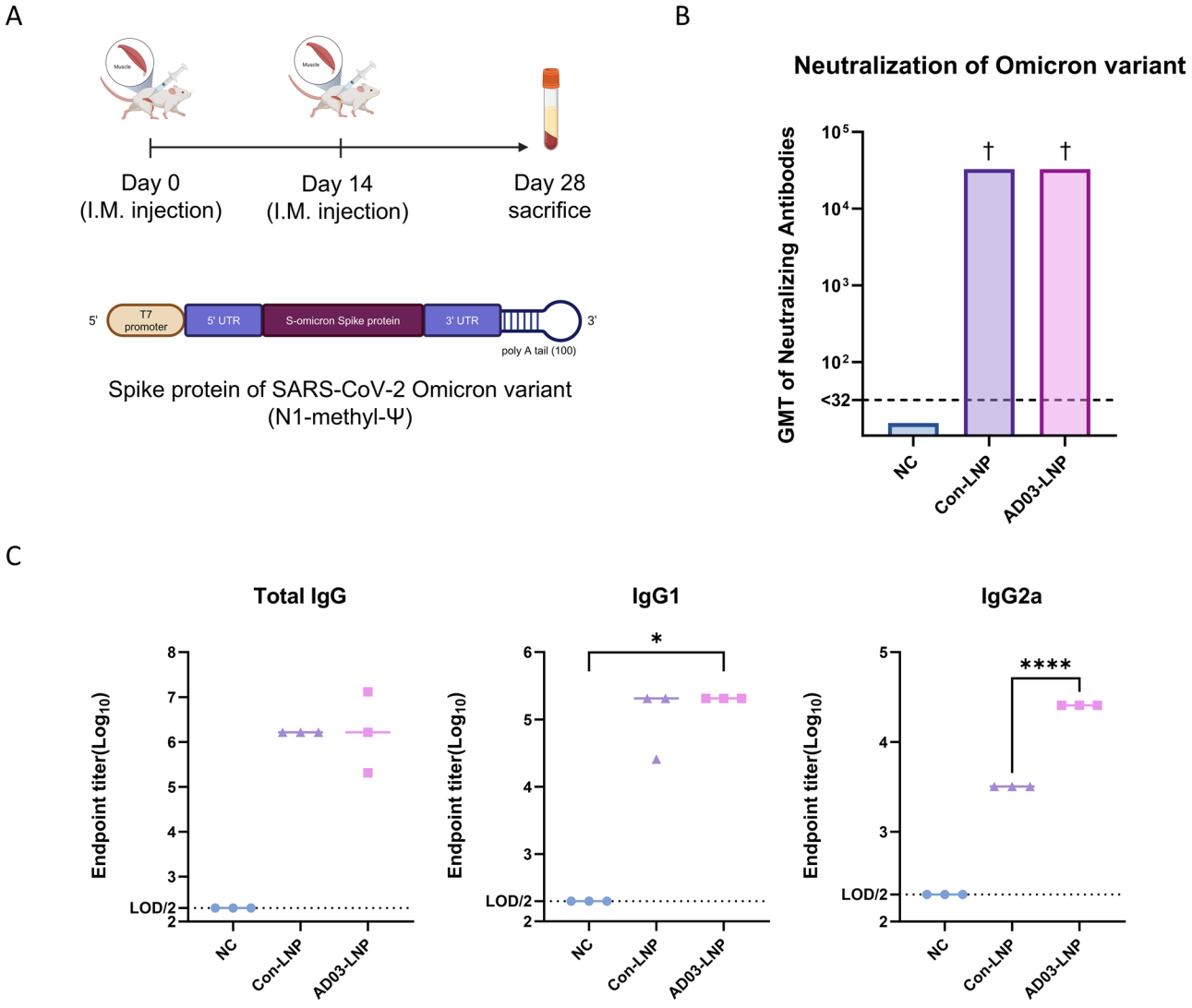



**Fig. 4** Neutralizing and antigen-specific IgG subclass responses following immunization. **(A)** Schematic of the immunization schedule. Balb/c female mice ($n = 5$ per group) were injected intramuscularly with 10 μg of S-omicron spike protein mRNA-lipid nanoparticles (LNPs) on day 0 (prime) and boosted on day 14. Whole blood was collected on day 28 for analysis. Serum samples were pooled and measured in technical triplicates. **(B)** Neutralizing antibody titers against the severe acute respiratory syndrome coronavirus 2 (Omicron strain) were assessed using day 28 serum samples. Titers are presented as geometric mean titers (GMTs), and the assay was performed with a viral back titer of $10^3$ $TCID_{50}$/mL. Samples above the upper limit of detection (†) were plotted at the maximum value. **(C)** Antigen-specific total immunoglobulin (Ig) G, IgG1, and IgG2a titers in day 28 serum were measured using enzyme-linked immunosorbent assay. Data are presented as the mean ± standard deviation. All *P*-values were determined using a one-way analysis of variance. *$P < 0.05$, **$P < 0.01$, ***$P < 0.001$, and ****$P < 0.0001$

showed an increased frequency of effector memory $CD8^+$ T cells, as well as a higher proportion of activated $CD8^+$ T cells (Fig. 5B). Nevertheless, the proportion of effector memory $CD4^+$ T cells remained comparable between the groups. In contrast, $CD69^+$ $CD4^+$ T cell frequency was elevated in the AD03-LNP group, showing enhanced activation of $CD4^+$ T cells (Fig. 5B). These findings align with previous observations, further supporting the selective enhancement of $CD8^+$ T cell-mediated memory responses by AD03-LNP. Moreover, $CD8^+$ T cells from the AD03-LNP group secreted higher levels of pro-inflammatory cytokines, including IFN-γ and TNF-α, in response to antigen-specific stimulation, compared to those from the Con-LNP group (Fig. 5C). Notably, the memory B-cell in the AD03-LNP group were not reduced compared to the Con-LNP group, indicating that incorporation of the TLR7/8 agonist did not impair memory B-cell generation (Fig. 5D). Additionally, total IgG levels were significantly elevated in the AD03-LNP group; nonetheless, IgG1 and IgG2a levels remained comparable between the groups, maintaining a balanced IgG1/IgG2a ratio (Fig. 5E). These results show that AD03-LNP selectively enhances antigen-specific $CD8^+$ T cell responses while simultaneously augmenting the magnitude of the

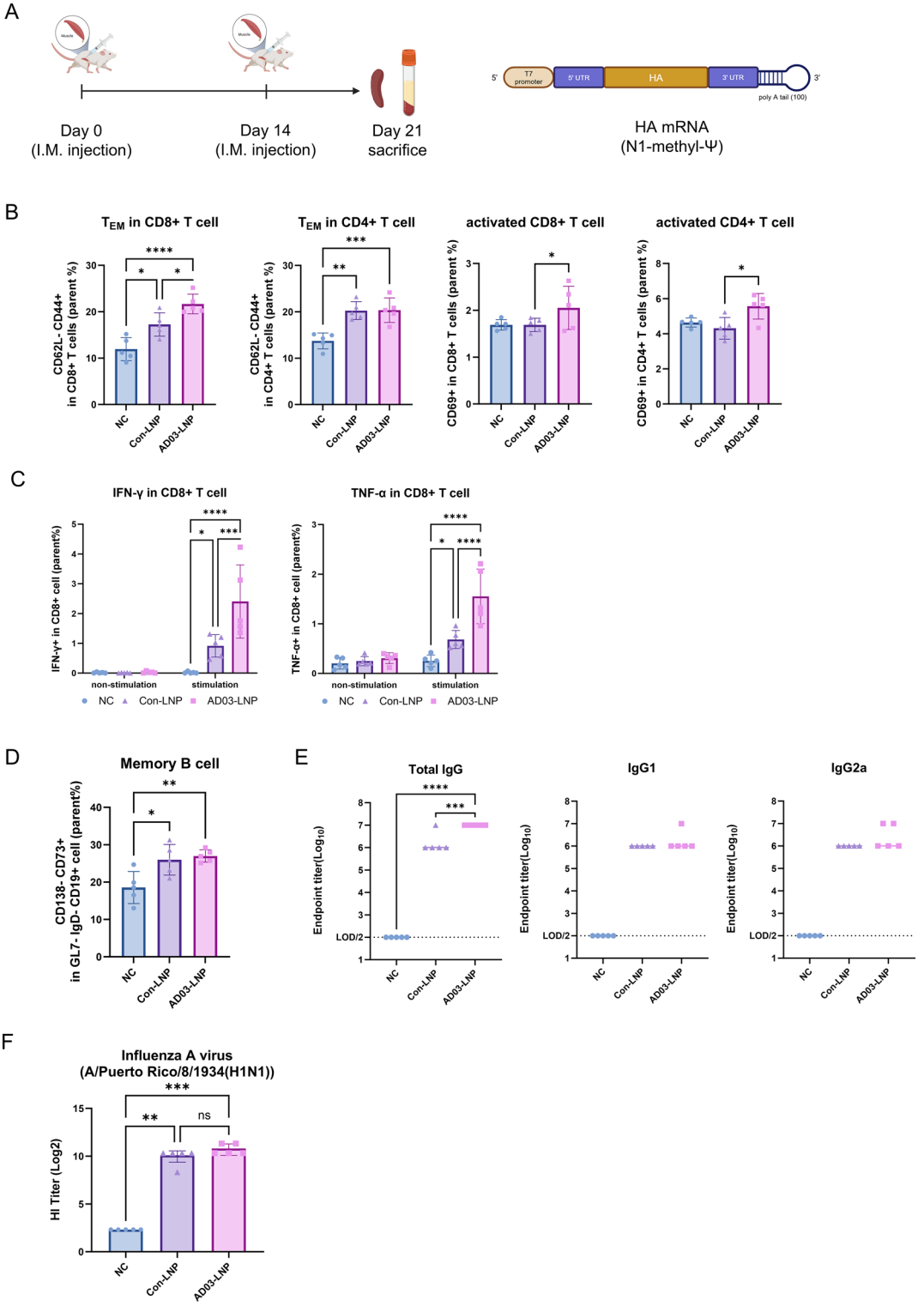



**Fig. 5** (See legend on next page.)

humoral response without compromising its quality or subclass balance, thereby supporting its potential to induce coordinated cellular and humoral immunity. This finding does not fully align with the previous observation that AD03-LNP preferentially enhanced IgG2a responses (Fig. 4C); however, the difference in IgG subclass distribution observed between day 7 and 14 post-boost likely reflects the temporal evolution of the germinal center

(See figure on previous page.)

**Fig. 5** Analysis of cellular and humoral immune responses using enzyme-linked immunosorbent assay and flow cytometry. **(A)** Schematic of the immunization schedule. Female BALB/c mice ($n = 5$ per group) aged 6 weeks were injected intramuscularly with 10 μg of hemagglutinin mRNA-lipid nanoparticles on day 0 (prime) and boosted on day 14. Whole blood and spleen were collected on day 21 for analysis. **(B)** The parent percentage of effector memory T cell ($T_{EM}$; $CD62L^-$, $CD44^+$) in CD8 + T cells, $T_{EM}$ ($CD62L^-$, $CD44^+$) in CD4 + T cells, $CD69^+$ cells in $CD8^+$ T cells, and $CD69^+$ cells in $CD4^+$ T cells. All data were analyzed using flow cytometry. **(C)** The parent percentage of interferon (IFN)-$\gamma^+$ cells and tumor necrosis factor (TNF)-$\alpha^+$ cells in $CD8^+$ T cells. All data were analyzed using flow cytometry. **(D)** The parent percentage of memory B cell (CD138- CD73 + in GL7- IgD- CD19+). All data were analyzed using flow cytometry. **(E)** Antigen-specific total immunoglobulin (Ig) G, IgG1, and IgG2a titers in day 21 serum were measured using enzyme-linked immunosorbent assay (ELISA). **(F)** Hemagglutination inhibition (HI) titers against vaccine strains were measured using the HI assay with serum obtained on day 21. All data are presented as the mean ± standard deviation. All *P*-values were determined using one-way ANOVA **(B, D-F)** and two-way ANOVA **(C)**. $^*P < 0.05$, $^{**}P < 0.01$, and $^{***}P < 0.001$

response. Here, Th1-driven IgG2a switching becomes more pronounced over time, suggesting that AD03-LNP continues to support Th1-type humoral immunity beyond the early post-vaccination phase. HI titers were comparably high in the Con-LNP and AD03-LNP groups, with no statistically significant differences observed, indicating robust neutralizing activity across formulations. (Fig. 5F).

To determine whether the enhanced $CD8^+$ T cell response observed in the AD03-LNP group was associated with changes in dendritic cell subsets, conventional dendritic cells (cDCs) distribution was further examined (Fig. S7). The cDC1/cDC2 ratio was significantly higher in the AD03-LNP group than in the Con-LNP group (Fig. S7A), showing preferential expansion or activation of cross-presenting dendritic cells. In parallel, the AD03-LNP group showed an increased population of short-lived effector cells (SLEC) within the CD8 + T cell (Fig. S7B), suggesting that the inclusion of a TLR7/8 agonist in the LNP formulation enhances antigen cross-presentation and promotes terminal differentiation of $CD8^+$ T cells through cDC1-mediated priming. Collectively, these findings show that AD03-LNP enhances T cell-mediated immunity without compromising antibody responses, which aligns with previous results. This finding supports the potential of AD03-LNP as a TLR7/8 agonist-integrated LNP mRNA vaccine capable of promoting robust antigen-specific T cell immunity while preserving humoral responses, notwithstanding the immunization schedule or the encoded antigen.

### Toll-like receptor agonist did not induce severe toxicity as determined via blood chemistry analysis and hematology analysis

To evaluate potential systemic toxicity and recovery after immunization, mice were administered 10 μg of HPV mRNA formulated in either Con-LNP or AD03-LNP through intramuscular injection on days 0 and 7. Body weight was measured at regular intervals following immunization. The Con-LNP and AD03-LNP groups showed transient weight loss immediately after immunization (Fig. 6A). However, body weights returned to baseline levels within 2–3 days, indicating a comparable response in both formulations (Fig. 6A).

To evaluate the potential toxicity due to TLR7/8 agonist-integrated LNPs, the serum samples were collected one week after the booster dose. Various biochemical markers were analyzed, including Serum alanine transaminase (ALT), aspartate transaminase (AST), total bilirubin (T-Bil), and creatinine (Crea) levels. All blood chemistry analyses showed no signs of severe toxicity (Fig. 6B).

Complete blood counts (CBCs) were conducted, including measurements of Red Blood Cell (RBC), Hemoglobin (HGB), Hematocrit (HCT), Reticulocyte (Retic), Platelet (PLT), and White Blood Cell (WBC) to further monitor hematological responses and detect potential systemic toxicity. Six-week-old female BALB/c mice were immunized intramuscularly on days 0 and 14 with 10 μg of HA mRNA formulated with either Con-LNP or AD03-LNP, and whole blood was collected on day 21, one week after the booster dose.

CBC analysis showed no significant differences in hematological parameters, including RBC, HGB, HCT, Reticulocytes, PLT, and WBC, between the Con-LNP and AD03-LNP groups, suggesting that the LNP formulations did not induce hematological toxicity (Fig. 6C).

## Discussion

N1-Methyl-Ψ, a representative example of modified UTP, is a groundbreaking invention in mRNA technology that earned Katalin Karikó a Nobel Prize [25]. Recent findings show that unmodified mRNA is rapidly degraded by TRIM25 in acidic environments, underscoring the importance of using modified nucleosides in mRNA vaccines [26].

This modification helps evade TLR7-mediated detection, which suppresses innate immune responses, thereby enhancing mRNA vaccine performance, reducing vaccine-related side effects, and increasing protein expression levels [7]. However, modified UTP can also result in diminished immune responses to mRNA vaccines and even tolerance against target antigens [27].

To this end, a formulation strategy in which a portion of cholesterol in the conventional LNP composition was replaced with a novel TLR7/8 agonist (AD7/8), aiming to enhance the immune response of mRNA vaccines without compromising their expression efficiency, was

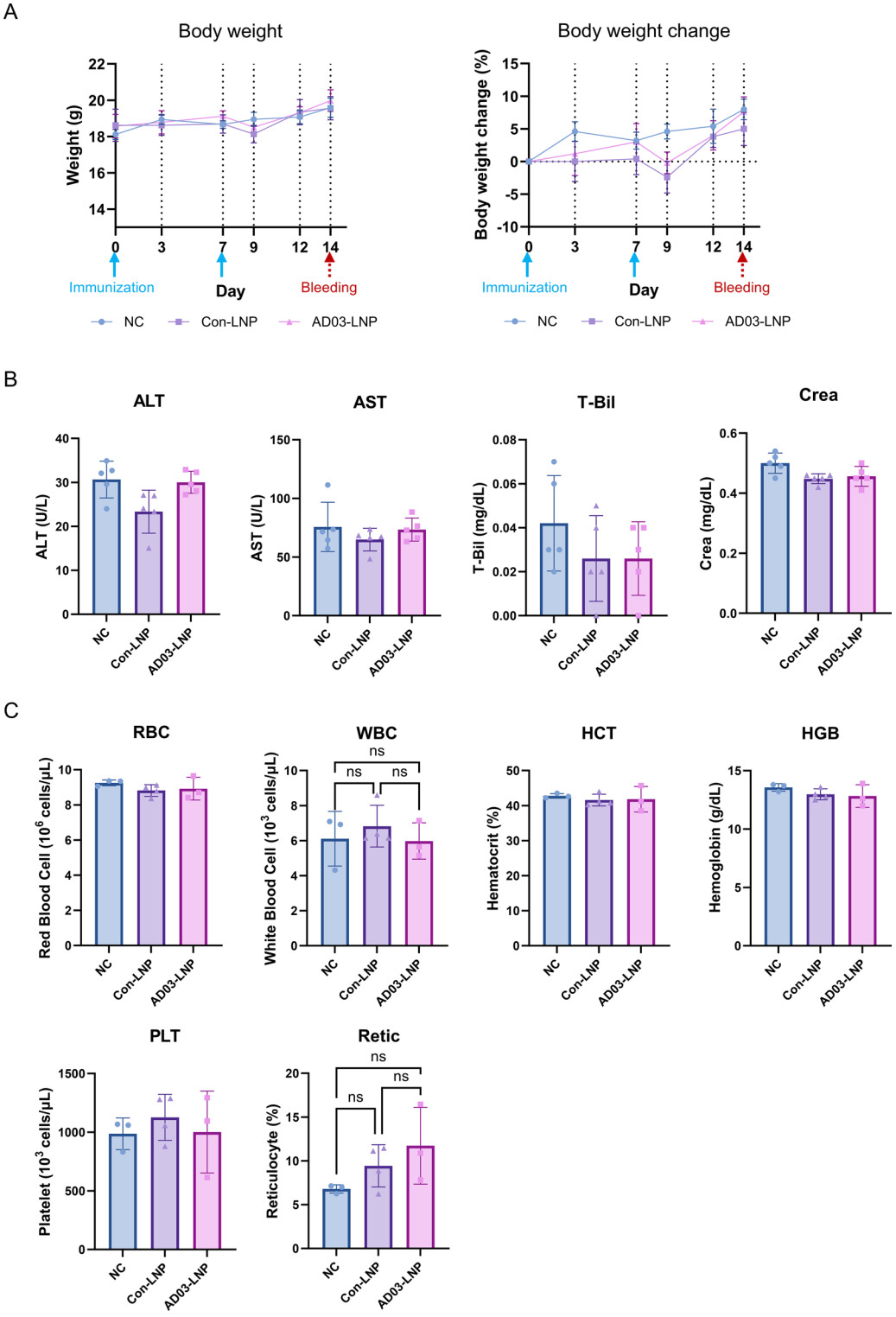



**Fig. 6** Blood biochemistry evaluation following lipid nanoparticle administration. **(A)** 6-week-old female C57BL mice ($n = 5$ per group) were administered HPV mRNA with Con-LNP or AD03-LNP via IM injection on days 0 and 7. Body weight was monitored to assess systemic toxicity. **(B)** Alanine transaminase (ALT), aspartate transaminase (AST), total bilirubin (T-Bil), and creatinine (Crea) levels were measured in serum collected 7 days after the booster injection of HPV mRNA-lipid nanoparticles. **(C)** Red blood cell (RBC), hemoglobin (HGB), hematocrit (HCT), reticulocyte (Retic), platelet (PLT), and white blood cell (WBC) levels were measured in whole blood collected 7 days after the booster injection of hemagglutinin (HA) mRNA-lipid nanoparticles. All data are presented as mean ± standard deviation **(A-C)**

employed. Within this formulation strategy, this agonist harmonized with mRNA-LNPs without hampering the LNP formulation stability. Although the mechanism was not explicitly addressed, the preserved or slightly enhanced expression efficiency observed in TLR7/8 agonist-incorporating LNPs is consistent with previous studies using R848-derived adjuvant lipidoids in lipid nanoparticles [12]. Since AD03-LNP consistently preserved or enhanced mRNA expression regardless of nucleoside type, one possible explanation is that cholesterol adjustment, together with TLR7/8 agonist incorporation, might have subtly altered the LNP composition in a way that could influence endosomal escape [12, 19]. In this context, how partial substitution of cholesterol with a TLR7/8 agonist in the LNP formulation preserves or modestly enhances mRNA translation remains unclear and warrants further investigation. Nevertheless, compared with previously reported LNP strategies employing R848-derived adjuvant lipidoids, in which covalent conjugation of R848 to lipid molecules often led to unpredictable release and reduced formulation flexibility [28], this approach integrates the novel TLR7/8 agonist AD7/8 into the LNP composition through partial cholesterol substitution, thereby maintaining physicochemical stability and enabling a more predictable immune activation profile. Moreover, it offers a simpler yet effective means to incorporate a TLR7/8 agonist into clinically established SM-102-based mRNA-LNP platform.

The study results showed that LNPs incorporating the TLR7/8 agonist significantly enhance antigen-specific CD8 + T cell responses. This result aligns with previous studies demonstrating that stimulation of innate immunity with unmodified mRNA can modulate T cells and enhance antitumor T cell immunity [11, 29]. Nevertheless, unmodified mRNA may lead to significantly reduced expression levels and antigen-specific antibody responses while also possibly inducing unintended excessive inflammatory reactions [6, 11, 29, 30]. Moreover, unmodified mRNA increases antigen-presenting $CD8^+$ T cells but does not significantly affect $CD4^+$ T cells [31]. Conversely, this and other studies showed that incorporating TLR7/8 agonists into LNPs not only increases antigen-specific $CD8^+$ T cells and cytokines (IFN-γ and TNF-α) associated with antitumor efficacy [32], but also slightly increases $CD4^+$ T cell activation. Thus, incorporating a TLR7/8 agonist into LNPs with N1-methyl-Ψ mRNA can amplify antigen-specific $CD8^+$ T cell responses through innate immune stimulation, similar to the antitumor effects observed with wild-type UTP mRNA, but without the drawbacks associated with unmodified nucleotides. Moreover, additional activation of $CD4^+$ T cells may provide an advantage in personalized cancer vaccines (PCVs), where robust $CD4^+$ T cell responses are essential for effective antitumor immunity [33, 34].

Furthermore, the comparison between the control LNP and TLR7/8 agonist-integrated LNP groups, analyzed two weeks after the booster immunization, showed no significant differences in antigen-specific total IgG responses or IgG1 levels, which are indicative of Th2 responses. However, the TLR7/8 agonist-integrated LNP group showed higher IgG2a levels, reflecting an enhanced Th1 response. This Th1 response enhancement shows a potential advantage in promoting antigen-specific memory T cell formation, which may contribute to stronger long-term protective immunity [35].

This strategy could improve resistance to reinfection and reduce the likelihood of tumor recurrence compared with conventional mRNA vaccines [36, 37], highlighting its potential for the future development of mRNA-based cancer vaccines. Moreover, it induces a strong antigen-specific Th1 response while maintaining high neutralizing antibody titers, suggesting potential for optimizing the design of viral and infectious disease vaccines to achieve robust cellular and humoral immunity [38]. Nonetheless, further studies are required to determine its impact on therapeutic efficacy.

Another notable finding of this study is that early and late humoral immune responses differ when TLR7/8 agonists are incorporated into lipid nanoparticles. One week after the booster immunization, the AD03-LNP group showed increased total IgG levels compared to the Con-LNP group, while maintaining a balanced IgG1/IgG2a ratio. This suggests that incorporating a TLR7/8 agonist can enhance the magnitude of the humoral response without skewing the Th1/Th2 polarization of antibody subclasses at early time points. Neutralizing activity remained comparable between the groups, indicating that TLR7/8 agonist incorporation enhanced the magnitude of the humoral response without impairing its neutralizing efficacy. Taken together with the observed increase in IgG2a levels at two weeks post-boost, these results show that AD03-LNP may promote a shift toward a Th1-biased humoral profile over time [39].

TLR agonists can induce systemic toxicity due to uncontrolled cytokine release, while the local administration of free TLR7 agonists can elevate levels of AST and ALT, indicating potential hepatotoxicity [40]. In this study, AD03-LNP resulted in no detectable signs of hepatotoxicity or nephrotoxicity, indicating a safety profile comparable to Con-LNP. This finding is noteworthy, as it indicates that incorporation of a TLR7/8 agonist into LNPs does not confer detectable toxicity risk.

In addition, both thermal stability and long-term storage remain recognized challenges for the broad application of mRNA-LNP formulations [41]. In this study, AD7/8-loaded LNPs stored at 4 °C for 14 days showed no significant differences in size, PDI, or EE% compared with day 0 or day 1 samples, and both Con-LNP and

AD03-LNP retained these properties after 5 months at 4 °C. Short-term storage at – 80 °C and 25 °C also preserved size and EE% for up to 7 days. These findings suggest that incorporation of the TLR7/8 agonist does not compromise formulation stability. However, only physicochemical parameters were evaluated, not biological activity such as mRNA expression efficiency or immunogenicity, which represents a limitation. Notably, previous studies have reported that, although physicochemical attributes and the amount of mRNA retained within LNPs remain unchanged after 7 days of storage at 4–25 °C, transgene expression is reduced relative to material stored under frozen conditions, underscoring the need for frozen storage [42]. Accordingly, future work should establish functional stability under long-term storage regimens to better support the commercialization potential of this LNP formulation.

## Conclusions

Partial replacement of cholesterol with a TLR7/8 agonist in LNP formulations significantly enhanced mRNA vaccine efficacy across multiple models, markedly increasing $CD8^+$ T cell responses and antibody production while maintaining neutralizing antibody titers. These immune responses were accompanied by elevated IFN-γ and TNF-α production and a higher proportion of effector memory $CD8^+$ T cells, indicating potential to both prevent severe viral infection and improve the efficacy of therapeutic cancer vaccines. Although physicochemical stability was preserved under different storage conditions, further studies are needed to establish functional stability and safety. Importantly, this strategy may address a key limitation of current mRNA vaccines, as strong humoral responses are induced but $CD8^+$ T cell immunity is often limited, particularly in older adults [43]. Collectively, these findings demonstrate that incorporating a TLR7/8 agonist into LNP formulations enhances mRNA vaccine efficacy while maintaining stability, offering a promising strategy for both therapeutic and prophylactic vaccines that require robust T cell responses.

## Supplementary Information

The online version contains supplementary material available at https://doi.org/10.1186/s13036-025-00573-1.

Supplementary Material 1

**Acknowledgements**
All individuals who contributed to the research and writing of the manuscript are listed as authors.

**Author contributions**
Conceptualization: H.C., H.K., S.B.H., J.-H.N.; Methodology: H.C., S.L., S.-H.B.; Investigation: H.C., S.L., S.-H.B., S.J. (Sohee Jo), J.K., Y.L., D.H., A.O., S.Y., S.J. (Sanghyuk Jeon), Y.-S.L., Y.C., S.C., G.R., S.L.; Data Curation: H.C., S.L., S.-H.B., S.J. (Sohee Jo), J.K., Y.L., D.H., A.O., S.Y., Y.-S.L., Y.C., S.C., S.L., H.-J.P., J.L., D.S., S.-H.H.; Resources: H.K., J.G., S.B.H.; Validation: H.C., S.J. (Sanghyuk Jeon); Supervision: J.-H.N.; Writing—original draft: H.C., S.L., J.-H.N.; writing —review and editing: H.C., S.L., S.B.H., J.-H.N.

**Funding**
This work was supported by grants from the Ministry of Food and Drug Safety (Grant Numbers: 22213MFDS421 and RS-2025-02213409 to J.-H.N.; RS-2023-00217074 to J.L.), and by a grant from the Korea Health Technology R&D Project through the Korea Health Industry Development Institute (KHIDI), funded by the Ministry of Health and Welfare, Republic of Korea (Grant Numbers: RS-2024-00507060 and RS-2024-00507223 to H.-J.P.), by Korea Institute of Planning and Evaluation for Technology in Food, Agriculture and Forestry (IPET) through High-Risk Animal Infectious Disease Control Technology Development Program, funded by Ministry of Agriculture, Food and Rural Affairs (MAFRA)(RS-2024-00399808 to S.-H.H.). This work was also partially supported by the Korea Research Institute of Chemical Technology (KK2532-10 to S.B.H.) and the Brain Korea 21 Four Program. The funders played no role in the study design, data collection, analysis and interpretation of data, or the writing of this manuscript.

**Data availability**
All data used in this study are included in this paper and its supplementary files. The datasets supporting the findings of this study are available from the corresponding author upon request.

## Declarations

**Ethics approval and consent to participate**
This study was approved by the Institutional Animal Care and Use Committee (IACUC) of the Catholic University of Korea (Approval No. CUK-IACUC-2023-048-02).

**Consent for publication**
Not applicable.

**Competing interests**
The authors declare no competing interests.

**Author details**
[1]Department of Biotechnology, The Catholic University of Korea, Bucheon, Gyeonggi-Do, Republic of Korea
[2]BK21 Four Department of Biotechnology, The Catholic University of Korea, Gyeonggi-Do, Bucheon, Republic of Korea
[3]Infectious Diseases Therapeutic Research Center, Therapeutics and Biotechnology Division, Korea Research Institute of Chemical Technology (KRICT), Daejeon 34114, Republic of Korea
[4]Department of Medicinal Chemistry and Pharmacology, University of Science and Technology, Daejeon 34113, Republic of Korea
[5]School of Pharmacy, Sungkyunkwan University, Suwon 16419, Republic of Korea
[6]Department of Virology, College of Veterinary Medicine and Research Institute for Veterinary Science, Seoul National University, Seoul, Republic of Korea
[7]Department of Microbiology, College of Medicine, Ewha Womans University, Seoul 078040, Republic of Korea
[8]Department of Medical and Biological Sciences, The Catholic University of Korea, 43 Jibong-ro, Bucheon, Gyeonggi-do 14662, Republic of Korea

Received: 4 July 2025 / Accepted: 15 October 2025
Published online: 19 November 2025

**References**

1. Yang W, Cao J, Cheng H, Chen L, Yu M, Chen Y, Cui X. Nanoformulations targeting immune cells for cancer therapy: mRNA therapeutics. Bioact Mater. 2023;23:438–70.
2. Miao L, Zhang Y, Huang L. mRNA vaccine for cancer immunotherapy. Mol Cancer. 2021;20(1):41.
3. Svitkin YV, Cheng YM, Chakraborty T, Presnyak V, John M, Sonenberg N. N1-methyl-pseudouridine in mRNA enhances translation through

eIF2alpha-dependent and independent mechanisms by increasing ribosome density. Nucleic Acids Res. 2017;45(10):6023–36.
4. Kariko K, Muramatsu H, Welsh FA, Ludwig J, Kato H, Akira S, Weissman D. Incorporation of Pseudouridine into mRNA yields superior nonimmunogenic vector with increased translational capacity and biological stability. Mol Ther. 2008;16(11):1833–40.
5. Andries O, Mc Cafferty S, De Smedt SC, Weiss R, Sanders NN, Kitada T. N(1)-methylpseudouridine-incorporated mRNA outperforms pseudouridine-incorporated mRNA by providing enhanced protein expression and reduced immunogenicity in mammalian cell lines and mice. J Control Release. 2015;217:337–44.
6. Anderson BR, Muramatsu H, Nallagatla SR, Bevilacqua PC, Sansing LH, Weissman D, Kariko K. Incorporation of Pseudouridine into mRNA enhances translation by diminishing PKR activation. Nucleic Acids Res. 2010;38(17):5884–92.
7. Kariko K, Buckstein M, Ni H, Weissman D. Suppression of RNA recognition by Toll-like receptors: the impact of nucleoside modification and the evolutionary origin of RNA. Immunity. 2005;23(2):165–75.
8. Morais P, Adachi H, Yu YT. The critical contribution of Pseudouridine to mRNA COVID-19 vaccines. Front Cell Dev Biol. 2021;9:789427.
9. Verbeke R, Lentacker I, Wayteck L, Breckpot K, Van Bockstal M, Descamps B, Vanhove C, De Smedt SC, Dewitte H. Co-delivery of nucleoside-modified mRNA and TLR agonists for cancer immunotherapy: restoring the immunogenicity of Immunosilent mRNA. J Control Release. 2017;266:287–300.
10. Seneff S, Nigh G, Kyriakopoulos AM, McCullough PA. Innate immune suppression by SARS-CoV-2 mRNA vaccinations: the role of G-quadruplexes, exosomes, and MicroRNAs. Food Chem Toxicol. 2022;164:113008.
11. Sittplangkoon C, Alameh MG, Weissman D, Lin PJC, Tam YK, Prompetchara E, Palaga T. mRNA vaccine with unmodified uridine induces robust type I interferon-dependent anti-tumor immunity in a melanoma model. Front Immunol. 2022;13:983000.
12. Han X, Alameh MG, Butowska K, Knox JJ, Lundgreen K, Ghattas M, Gong N, Xue L, Xu Y, Lavertu M, et al. Adjuvant lipidoid-substituted lipid nanoparticles augment the immunogenicity of SARS-CoV-2 mRNA vaccines. Nat Nanotechnol. 2023;18(9):1105–14.
13. Islam MA, Rice J, Reesor E, Zope H, Tao W, Lim M, Ding J, Chen Y, Aduluso D, Zetter BR, et al. Adjuvant-pulsed mRNA vaccine nanoparticle for immunoprophylactic and therapeutic tumor suppression in mice. Biomaterials. 2021;266:120431.
14. Duan T, Du Y, Xing C, Wang HY, Wang RF. Toll-Like receptor signaling and its role in Cell-Mediated immunity. Front Immunol. 2022;13:812774.
15. Sun H, Li Y, Zhang P, Xing H, Zhao S, Song Y, Wan D, Yu J. Targeting toll-like receptor 7/8 for immunotherapy: recent advances and prospectives. Biomark Res. 2022;10(1):89.
16. Xing J, Zhao X, Li X, Fang R, Sun M, Zhang Y, Song N. The recent advances in vaccine adjuvants. Front Immunol. 2025;16:1557415.
17. Sanlorenzo M, Novoszel P, Vujic I, Gastaldi T, Hammer M, Fari O, De Sa Fernandes C, Landau AD, Gocen-Oguz BV, Holcmann M, et al. Systemic IFN-I combined with topical TLR7/8 agonists promotes distant tumor suppression by c-Jun-dependent IL-12 expression in dendritic cells. Nat Cancer. 2025;6(1):175–93.
18. Lesniak M, Lipniarska J, Majka P, Kopyt W, Lejman M, Zawitkowska J. The role of TRL7/8 agonists in cancer therapy, with special emphasis on hematologic malignancies. Vaccines (Basel) 2023, 11(2).
19. Luo C, Li Y, Liu H, He J, Yang X, Zhao E, Zi G, Liu L, Hong Y, Wang H, et al. Intracellular trafficking of lipid nanoparticles is hindered by cholesterol. Int J Pharm. 2025;671:125240.
20. Su K, Shi L, Sheng T, Yan X, Lin L, Meng C, Wu S, Chen Y, Zhang Y, Wang C, et al. Reformulating lipid nanoparticles for organ-targeted mRNA accumulation and translation. Nat Commun. 2024;15(1):5659.
21. Ganapathi L, Van Haren S, Dowling DJ, Bergelson I, Shukla NM, Malladi SS, Balakrishna R, Tanji H, Ohto U, Shimizu T, et al. The imidazoquinoline Toll-Like Receptor-7/8 agonist Hybrid-2 potently induces cytokine production by human newborn and adult leukocytes. PLoS ONE. 2015;10(8):e0134640.
22. Happ M, Bathke AC, Brunner E. Optimal sample size planning for the Wilcoxon-Mann-Whitney test. Stat Med. 2019;38(3):363–75.
23. Park HJ, Bang YJ, Kwon SP, Kwak W, Park SI, Roh G, Bae SH, Kim JY, Kwak HW, Kim Y, et al. Analyzing immune responses to varied mRNA and protein vaccine sequences. NPJ Vaccines. 2023;8(1):84.
24. Cheng Y, Borcherding N, Ogunsakin A, Lemke-Miltner CD, Gibson-Corley KN, Rajan A, Choi AB, Wongpattaraworakul W, Chan CHF, Salem AK, et al. The anti-tumor effects of cetuximab in combination with VTX-2337 are T cell dependent. Sci Rep. 2021;11(1):1535.
25. Gao Y, Yang L, Li Z, Peng X, Li H. mRNA vaccines in tumor targeted therapy: mechanism, clinical application, and development trends. Biomark Res. 2024;12(1):93.
26. Kim M, Pyo Y, Hyun SI, Jeong M, Choi Y, Kim VN. Exogenous RNA surveillance by proton-sensing TRIM25. Science. 2025;388(6742):eads4539.
27. Rubio-Casillas A, Cowley D, Raszek M, Uversky VN, Redwan EM. Review: N1-methyl-pseudouridine (m1Psi): friend or foe of cancer? Int J Biol Macromol. 2024;267(Pt 1):131427.
28. Qi S, Zhang X, Yu X, Jin L, Yang K, Wang Y, Feng Y, Lei J, Mao Z, Yu G. Supramolecular lipid nanoparticles based on Host-Guest recognition: A new generation delivery system of mRNA vaccines for cancer immunotherapy. Adv Mater. 2024;36(23):e2311574.
29. Fournier C, Mercey-Ressejac M, Derangere V, Al Kadi A, Rageot D, Charrat C, Leroy A, Vollaire J, Josserand V, Escude M, et al. Nanostructured lipid carriers based mRNA vaccine leads to a T cell-inflamed tumour microenvironment favourable for improving PD-1/PD-L1 blocking therapy and long-term immunity in a cold tumour model. EBioMedicine. 2025;112:105543.
30. Wang Z, Jacobus EJ, Stirling DC, Krumm S, Flight KE, Cunliffe RF, Mottl J, Singh C, Mosscrop LG, Santiago LA, et al. Reducing cell intrinsic immunity to mRNA vaccine alters adaptive immune responses in mice. Mol Ther Nucleic Acids. 2023;34:102045.
31. Oberli MA, Reichmuth AM, Dorkin JR, Mitchell MJ, Fenton OS, Jaklenec A, Anderson DG, Langer R, Blankschtein D. Lipid nanoparticle assisted mRNA delivery for potent cancer immunotherapy. Nano Lett. 2017;17(3):1326–35.
32. Jorgovanovic D, Song M, Wang L, Zhang Y. Roles of IFN-gamma in tumor progression and regression: a review. Biomark Res. 2020;8:49.
33. Salomon N, Vascotto F, Selmi A, Vormehr M, Quinkhardt J, Bukur T, Schrors B, Loewer M, Diken M, Tureci O, et al. A liposomal RNA vaccine inducing neoantigen-specific CD4(+) T cells augments the antitumor activity of local radiotherapy in mice. Oncoimmunology. 2020;9(1):1771925.
34. Huff AL, Longway G, Mitchell JT, Andaloori L, Davis-Marcisak E, Chen F, Lyman MR, Wang R, Mathew J, Barrett B et al. CD4 T cell-activating neoantigens enhance personalized cancer vaccine efficacy. JCI Insight 2023, 8(23).
35. Martinez V, Costagliola D, Bonduelle O, N'go N, Schnuriger A, Theodorou I, Clauvel JP, Sicard D, Agut H, Debre P, et al. Combination of HIV-1-specific CD4 Th1 cell responses and IgG2 antibodies is the best predictor for persistence of long-term nonprogression. J Infect Dis. 2005;191(12):2053–63.
36. Eko FO, Ekong E, He Q, Black CM, Igietseme JU. Induction of immune memory by a multisubunit chlamydial vaccine. Vaccine. 2011;29(7):1472–80.
37. Haabeth OA, Lorvik KB, Hammarstrom C, Donaldson IM, Haraldsen G, Bogen B, Corthay A. Inflammation driven by tumour-specific Th1 cells protects against B-cell cancer. Nat Commun. 2011;2:240.
38. Skibinski DA, Hanson BJ, Lin Y, von Messling V, Jegerlehner A, Tee JB, Chye de H, Wong SK, Ng AA, Lee HY, et al. Enhanced neutralizing antibody titers and Th1 polarization from a novel Escherichia coli derived pandemic influenza vaccine. PLoS ONE. 2013;8(10):e76571.
39. Miller SM, Cybulski V, Whitacre M, Bess LS, Livesay MT, Walsh L, Burkhart D, Bazin HG, Evans JT. Novel lipidated imidazoquinoline TLR7/8 adjuvants elicit influenza-Specific Th1 immune responses and protect against heterologous H3N2 influenza challenge in mice. Front Immunol. 2020;11:406.
40. Smith AAA, Gale EC, Roth GA, Maikawa CL, Correa S, Yu AC, Appel EA. Nanoparticles presenting potent TLR7/8 agonists enhance Anti-PD-L1 immunotherapy in cancer treatment. Biomacromolecules. 2020;21(9):3704–12.
41. Hashiba K, Taguchi M, Sakamoto S, Otsu A, Maeda Y, Ebe H, Okazaki A, Harashima H, Sato Y. Overcoming thermostability challenges in mRNA-lipid nanoparticle systems with piperidine-based ionizable lipids. Commun Biol. 2024;7(1):556.
42. Kamiya M, Matsumoto M, Yamashita K, Izumi T, Kawaguchi M, Mizukami S, Tsurumaru M, Mukai H, Kawakami S. Stability study of mRNA-lipid nanoparticles exposed to various conditions based on the evaluation between physicochemical properties and their relation with protein expression ability. Pharmaceutics 2022, 14(11).
43. Kometani K, Yorimitsu T, Jo N, Yamaguchi E, Kikuchi O, Fukahori M, Sawada T, Tsujimoto Y, Sunami A, Li M, et al. Booster COVID-19 mRNA vaccination ameliorates impaired B-cell but not T-cell responses in older adults. Front Immunol. 2024;15:1455334.

## Publisher's note

Springer Nature remains neutral with regard to jurisdictional claims in published maps and institutional affiliations.